Heterogeneous & Homogeneous & Bio- & Nano-

CHEMCATCHEM

CATALYSIS

Accepted Article

Title: Oxidation of cyclohexene in the presence of transition metal substituted phosphotungstates and hydrogen peroxide: catalysis and reaction pathways

Authors: Yuexiao Song, Feng Xin, Lexiang Zhang, and Yong Wang

This manuscript has been accepted after peer review and appears as an Accepted Article online prior to editing, proofing, and formal publication of the final Version of Record (VoR). This work is currently citable by using the Digital Object Identifier (DOI) given below. The VoR will be published online in Early View as soon as possible and may be different to this Accepted Article as a result of editing. Readers should obtain the VoR from the journal website shown below when it is published to ensure accuracy of information. The authors are responsible for the content of this Accepted Article.

To be cited as: *ChemCatChem* 10.1002/cctc.201700856

Link to VoR: http://dx.doi.org/10.1002/cctc.201700856

A Journal of ChemPubSoc Europe

WILEY-VCH

www.chemcatchem.org

Oxidation of cyclohexene in the presence of transition metal substituted phosphotungstates and hydrogen peroxide: catalysis and reaction pathways

Yuexiao Song, Feng Xin,* Lexiang Zhang, Yong Wang[a]

Abstract: Homogeneous catalytic oxidations of cyclohexene by transition metal substituted phosphotungstates $[PW_{11}M(L)O_{39}]^{m-}$ ($PW_{11}M$, M = Co(II), Cu(II), Fe(III), Ni(II), Mn(II), L = H_2O or absence) with hydrogen peroxide in acetonitrile were experimentally studied. The catalytic activities of allylic oxidation were found to strongly depend on the transition metals, and $PW_{11}Co$ showed the highest activity. The product distribution and the catalyst stability were dominated by mole ratio of hydrogen peroxide to $PW_{11}M$, whose low or high led to stable structure of $PW_{11}M$ and predominant formation of allylic oxidation products or decomposition of $PW_{11}M$. Different from the activation of allylic C–H bond by radicals, the oxidation of C=C double bond was based on tungsten-peroxo species. A reaction mechanism composed of radical and non-radical processes was proposed from nuclear magnetic resonance (NMR), electron paramagnetic resonance (EPR) and kinetic data, to describe the reaction pathways of cyclohexene oxidation.

Introduction

Allylic oxofunctionalization of cycloalkenes, represented by cyclohexene, is a promising process for the obtention of α,β-unsaturated alcohols and ketones (e.g., 2-cyclohexene-1-ol and 2-cyclohexene-1-one) which are valuable intermediates in manufacturing a variety of chemicals.[1–3] With much attention drawn toward the green chemistry, hydrogen peroxide (H_2O_2) or molecular oxygen (O_2) is used as a mono-oxygen source to accomplish allylic oxidations since they are economically and environmentally desirable oxidants, and produce water as the sole by-product.[2–5] Therefore, various kinds of complexes of transition metals, e.g., Au,[2,6,7] Co,[5,8] Cr,[1,9] Cu,[3,10–12] Fe,[4,5] Mn,[13] etc., have been developed for catalytic oxidation of cycloalkenes with H_2O_2 or O_2 in recent decade. In practice, during the oxidation of cycloalkenes, allylic oxidation and epoxidation are often competitive processes and occur simultaneously.[14] Compared with epoxidation, allylic oxidation preserves the C=C double bond in the products and allows further useful transformations.[12,14] Hence, catalytic activity and selectivity in allylic oxidation are two key points of interest in the research.

The allylic oxidation of cycloalkenes proceeds via a radical mechanism[1,7,11,15,16] and it tends to occur with low oxidation state transition metals as active catalyst[14,17]. Transition metal substituted polyoxometalates (TMSPs) with reactive low valent transition metal centers are fascinating catalysts for the transformation of hydrocarbons into oxygenated derivatives due to high capacity as oxygen transfer agents.[18–20] To date, many good examples of TMSPs based catalytic systems have been well documented.[21] Amongst the numerous polyoxometalate catalysts, the Keggin-type TMSPs have been extensively researched in homogeneous and heterogeneous catalysis for oxidative reactions using H_2O_2 as the oxygen donor, like hydroxylation of alkanes,[22–26] epoxidation of alkenes,[19,20,27–29] oxidation of styrene[30–33] and alcohols[34].

To our knowledge, only a few publications involving allylic oxidation can be found about the oxidation of cycloalkenes catalyzed by TMSPs with H_2O_2 or O_2.[22,35–40] Mizuno et al. described the oxidation of several alkenes catalyzed by *di*-iron-substituted silicotungstate $[\gamma\text{-}SiW_{10}\{Fe(OH_2)\}_2O_{38}]^{6-}$ with a high efficiency of H_2O_2 utilization.[22,35] Kholdeeva et al. published the oxidation of cyclohexene in the presence of titanium-substituted phosphotungstate $[PW_{11}TiO_{40}]^{5-}$ and H_2O_2.[36–38] Maksimchuk and co-workers immobilized $[PW_{11}Co(H_2O)O_{39}]^{5-}$ on MIL-101[38] and NH_2-modified mesoporous silicate matrixes[39] to realize the oxidation of *α*-pinene with O_2. Verbenol and verbenone were formed as the major products over the supported $[PW_{11}Co(H_2O)O_{39}]^{5-}$ catalysts during the autoxidation of *α*-pinene, while *α*-pinene epoxide was produced with 94% selectivity at 96% conversion when *α*-pinene was co-oxidized with isobutyraldehyde.[39] However, these catalytic systems researched mainly focused on the epoxidation reactions or the properties of catalyst itself, and showed poor catalytic activity and selectivity in allylic oxidation. In addition, the mechanism of allylic oxidation catalyzed by TMSPs remains unknown, and the effect of H_2O_2 on the stability of TMSPs is usually ignored. Recently, $H_{3+x}PMo_{12-x}V_xO_{40}$ (x = 1, 2)/metal-organic framework hybrids were prepared by a direct hydrothermal method for catalyzing the allylic oxidation of cyclohexene.[40]

In this work, we describe the oxidation of cyclohexene with aqueous H_2O_2 in acetonitrile, catalyzed by the Keggin-type transition metal mono-substituted phosphotungstates $[PW_{11}M(L)O_{39}]^{m-}$ ($PW_{11}M$), M = Co(II), Cu(II), Fe(III), Ni(II), Mn(II) L = H_2O or absence. The selectivity to allylic oxidation products strongly depends on the transition metals and the mole ratio of H_2O_2 to $PW_{11}M$. A particular attention is given to investigate the catalytic stability of $PW_{11}M$ and the reaction pathways of allylic oxidation and epoxidation. The transformation of $PW_{11}M$ (M = Co, Cu, Ni and Mn) similar to $[PW_{11}O_{39}]^{7-}$ (PW_{11})[41,42] and $[PW_{12}O_{40}]^{3-}$ (PW_{12})[43–45] in the presence of excess H_2O_2 was observed as shown in Scheme 1, which had profound effects on product selectivity.

[a] Y. Song, Prof. F. Xin, L. Zhang, Y. Wang
School of Chemical Engineering and Technology
Tianjin University
Tianjin, 300350 (P.R. China)
E-mail: xinf@tju.edu.cn

Supporting information for this article is given via a link at the end of the document.

Accepted Manuscript

This article is protected by copyright. All rights reserved.

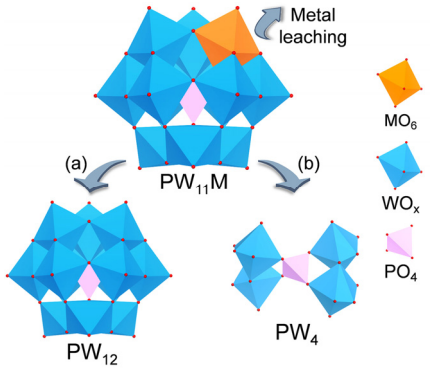

Scheme 1. Schematic representation of the transformation of $PW_{11}M$ in the presence of 250 equivalents of H_2O_2: (a) for M = Co, Cu, Ni and Mn, (b) for M = Co, Ni and Mn.

Results and Discussion

Oxidation of cyclohexene

The oxidation of cyclohexene was carried out with H_2O_2 in homogeneous phase using acetonitrile as solvent. The results for oxidation of cyclohexene catalyzed by phosphotungstates are presented in Table 1 along with the results of blank experiment. Oxidation reactions occurred both in allylic C–H bonds and C=C double bond (Scheme 2). Allylic oxidation gave 2-cyclohexen-1-ol (**1**), 2-cyclohexen-1-one (**2**) and cyclohexene hydroperoxide (**3**) as major products. Cyclohexene oxide (**4**), *trans*-cyclohexanediol (**5**), 2-hydroxycyclohexan-1-one (**6**) and adipaldehyde (**7**) were formed as products of oxidation of the C=C double bond. As the deeper oxidation products, **6** and **7** were undetected or neglected in related research.[1–12] All of the products except cyclohexene hydroperoxide (**3**) were identified by GC-MS technique. The yield details of each product based on cyclohexene are listed in Table S1 in the Supporting Information.

A blank experiment (Table 1, entry 1) showed that cyclohexene oxidation slowly proceeded in the absence of catalyst under the conditions employed when H_2O_2 was used as oxidant, while there was no product detected under mild conditions using O_2 as oxidant.[1,12] But the uncatalyzed oxidation of cyclohexene with O_2 was also found under higher temperature and oxygen pressure conditions.[5,7,9] In both cases, the allylic oxidation predominantly occurred during the uncatalyzed oxidation of cyclohexene.

For $PW_{11}M$ (M = Co, Cu, Fe, Ni and Mn), the product distribution, substrate conversion and H_2O_2 efficiency acquired strongly depended on the transition metal centers. As shown in Table 1, except for $PW_{11}Ni$, the hydroperoxide **3** was the dominant allylic oxidation product under all conditions. Similarly, substantial amounts of alkyl hydroperoxides were given in the oxidation of alkanes catalyzed by transition metal complexes with H_2O_2, in addition to usually smaller concentrations of alcohols and ketones.[46,47] Both $PW_{11}Co$ and $PW_{11}Cu$ showed

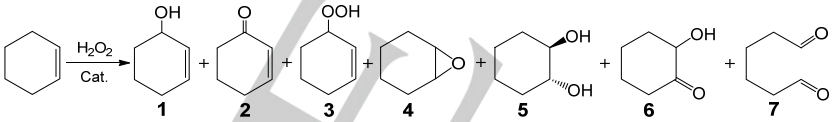

Scheme 2. Products of cyclohexene oxidation catalyzed by phosphotungstates at 60 °C

Table 1. Oxidation of cyclohexene catalyzed by phosphotungstates with H_2O_2.[a]

Entry	Catalyst	Selectivity of products [%]					$Y_{allylic}$ [%][d]	$C_{cyclohexene}$ [%][e]	E_{H2O2} [%][f]
		1	**2**	**3**	Others[b]	$S_{allylic}$[c]			
1	–	17.0	53.2	12.7	17.1	82.9	2.4	0.8	99.0
2	$PW_{11}Co$	12.9	25.2	48.2	13.7	86.3	59.7	19.0	70.1
3	$PW_{11}Cu$	15.7	17.0	60.7	6.6	93.4	34.0	10.0	35.3
4	$PW_{11}Fe$	6.3	17.0	20.7	56.0	44.0	31.1	19.0	75.5
5	$PW_{11}Ni$	1.9	4.8	2.1	91.2	8.8	10.9	35.4	98.0
6	$PW_{11}Mn$	0.6	1.8	24.0	73.6	26.4	6.2	5.9	15.0
7	PW_{11}	0.3	3.2	12.6	83.9	16.1	20.9	33.0	80.1
8	PW_4	0.5	1.8	3.8	93.9	6.1	9.6	41.7	96.8
9	PW_{12}	7.3	27.8	8.4	56.5	43.5	5.1	3.6	98.4

[a] Reaction conditions: catalyst (40 μmol), cyclohexene (20 mmol), H_2O_2 (10 mmol), CH_3CN (10 mL), 60 °C, 3 h. [b] Sum of selectivities to **4**, **5**, **6** and **7**. [c] Selectivity of allylic oxidation products (**1**, **2** and **3**). [d] Yield of allylic oxidation products was determined by GC based on H_2O_2, 100 × (moles of **1** + 2 × moles of **2** and **3**)/moles of initial H_2O_2. [e] Conversion was determined by GC based on cyclohexene, 100 × moles of products/moles of initial cyclohexene. [f] Efficiency of H_2O_2 utilization, 100 × (moles of **1**, **4** and **5** + 2 × moles of **2**, **3**, **6** and **7**)/moles of H_2O_2 consumed.

Accepted Manuscript

This article is protected by copyright. All rights reserved.

good catalytic selectivities to allylic oxidation, and the sum of selectivities to 1, 2 and 3 were 86.3% and 93.4%, respectively (Table 1, entries 2 and 3). However, $PW_{11}Co$ afforded about twice higher yield of allylic oxidation products than $PW_{11}Cu$, and showed the highest catalytic activity in allylic oxidation among $PW_{11}M$. Interestingly, mono-Co-substituted polyoxometalates appeared more effective than other metal substituted analogues in oxidative reactions, like the oxidation of styrene to benzaldehyde; no matter they were mono-substituted phosphotungstates ($PW_{11}M$), phosphomolybdates ($PMo_{11}M$), or silicotungstates ($SiW_{11}M$).[19,30,32] The transition metal centers appeared to play an important role in the catalytic performance. Although $PW_{11}Fe$ and $PW_{11}Ni$ provided 19.0% and 35.4% of cyclohexene conversion respectively (Table 1, entries 4 and 5), cyclohexene oxide (**4**) and its derivatives (**5**, **6** and **7**) were mainly produced.

It is well known that H_2O_2 is decomposed into H_2O and O_2 in some extent during the transition metal-catalyzed H_2O_2 based oxidation reactions.[23,44] The efficiency for the utilization of H_2O_2 in the presence and absence of phosphotungstates is listed in Table 1, which had a critical influence on the oxidation efficiency. All phosphotungstates appeared to accelerate the undesirable decomposition of H_2O_2. Especially for $PW_{11}Mn$ (Table 1, entry 6), it showed a much lower cyclohexene conversion than other $PW_{11}M$ due to the only 15.0% efficiency of H_2O_2 utilization.

For comparison, catalytic performance of PW_{11}, PW_4 and PW_{12} were studied under the same conditions (Table 1, entries 7, 8 and 9). $\{PO_4[WO(O_2)_2]_4\}^{3-}$ is postulated to be the active oxygen-transfer species in Ishii-Venturello systems,[21,44,48] and it has been isolated and characterized crystallographically[49]. Ishii-Venturello systems are highly efficient for the epoxidation of alkenes with polyoxometalate catalysts and H_2O_2 oxidant.[50,51] In this work, $\{PO_4[WO(O_2)_2]_4\}^{3-}$ was synthesized as tetrabutylammonium salt using $H_3PW_{12}O_{40}$ as the precursor and H_2O_2 as the oxidant.[43] However, PW_{12} afforded only 2.0% of total yield of **4** and **5** based on cyclohexene (Table 1, entry 9). It showed poor catalytic activity in epoxidation of cyclohexene. $[PW_{11}O_{39}]^{7-}$ was proved to be another kind of precursor used to catalyze alkene epoxidations and alcohol oxidations with H_2O_2.[41,42] The total selectivity to cyclohexene oxide (**4**) and its derivatives (**5**, **6** and **7**) attained 83.9% at 33.0% conversion and 93.9% at 41.7% conversion catalyzed by PW_{11} and PW_4, respectively. Moreover, it is worth noting that PW_{11} and PW_4 also produced the hydroperoxide **3** as the dominant allylic oxidation product.

Effect of H_2O_2 to $PW_{11}M$ mole ratio. To evaluate the effect of H_2O_2 on the oxidation of cyclohexene, experiments were conducted by two strategies. First, the H_2O_2 to $PW_{11}Co$ mole ratios were changed from 3333 to 500 by varying the amount of $PW_{11}Co$ and keeping the amount of H_2O_2 constant. Second, we varied the amount of H_2O_2 and fixed the amount of $PW_{11}Co$ (40 μmol). As shown in Figure 1, it was beneficial to the selectivity to allylic oxidation products with the decrease in the mole ratio of H_2O_2 to $PW_{11}Co$ for both strategies, but the latter strategy showed more significant influence on cyclohexene oxidation than the former one.

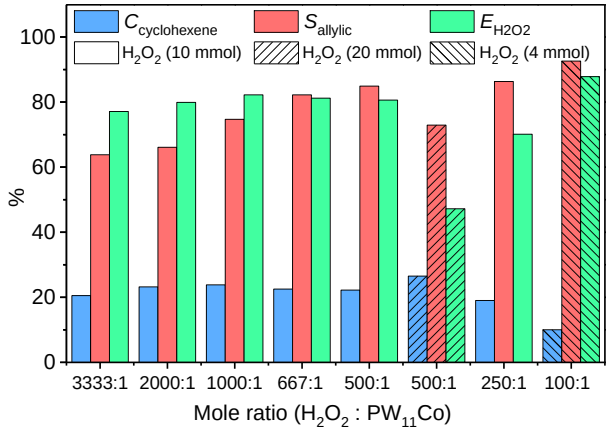

Figure 1. Effect of mole ratio on cyclohexene oxidation catalyzed by $PW_{11}Co$; $C_{cyclohexene}$, conversion was based on cyclohexene; $S_{allylic}$, selectivity of allylic oxidation products; E_{H2O2}, efficiency of H_2O_2 utilization. Reaction conditions: $PW_{11}Co$ (3–40 μmol), cyclohexene (20 mmol), CH_3CN (10 mL), 60 °C, 3 h.

For the first strategy, the amount of $PW_{11}Co$ could affect the efficiency of H_2O_2 utilization, while showed little effect on cyclohexene conversion. When the amount of $PW_{11}Co$ was greater than or equal to 10 μmol (H_2O_2:$PW_{11}Co$ ≤ 1000:1), the decrease in the amount of $PW_{11}Co$ benefited the utilization of H_2O_2, even though the H_2O_2 to $PW_{11}M$ mole ratios increased. It achieved over 80% efficiency of H_2O_2 utilization using 10–20 μmol $PW_{11}Co$. For the second strategy, by increasing the mole ratio from 100 to 500, the cyclohexene conversion increased from 10.0% to 26.5%, but the selectivity to allylic oxidation products sharply decreased from 92.6% to 72.9%. Much more significant decrease of the selectivity from 94.1% to 10.4% could be observed for $PW_{11}Mn$ (Figure S2d in the Supporting Information). Meanwhile, $PW_{11}Cu$, $PW_{11}Fe$ and $PW_{11}Ni$ showed the similar trends (Figure S2 in the Supporting Information). Based on these results, a conclusion could be drawn that the increase in the H_2O_2 to $PW_{11}M$ mole ratio benefited the oxidation of C=C double bond in the presence of $PW_{11}M$. Indeed, much higher selectivity and yield of cyclohexene oxide (**4**) and its derivatives (**5**, **6** and **7**) were formed under higher H_2O_2 to $PW_{11}M$ mole ratio conditions. Specially, for $PW_{11}Cu$, increasing the mole ratio from 250 to 500 resulted in a dramatic change in cyclohexene conversion and efficiency of H_2O_2 utilization (Figure S2a in the Supporting Information). The decomposition of H_2O_2 significantly occurred as a side reaction under high concentration of H_2O_2 catalyzed by $PW_{11}Cu$. The efficiency of H_2O_2 utilization decreased as the mole ratio increased for $PW_{11}Cu$, $PW_{11}Co$, $PW_{11}Fe$ and $PW_{11}Ni$ which was different from the first strategy. In contrast, $PW_{11}Mn$ afforded an increased efficiency of H_2O_2 utilization under the mole ratio of 500:1, and an increased cyclohexene conversion under the mole ratio of 100:1 (Figure S2d in the Supporting Information). Substrate oxidation and H_2O_2 decomposition are two competitive processes using H_2O_2 as oxidant. Substrate conversion and efficiency of H_2O_2 utilization will be determined by the dominant one.

Accepted Manuscript

This article is protected by copyright. All rights reserved.

Catalyst stability

Thermal stability, hydrolytic stability and oxidative stability are usually concerned in the research of polyoxometalate catalysts.[21] The thermal decomposition of $PW_{11}M$ has been well investigated by Gamelas et al.[52] Decomposition behaviors observed in this work were in agreement with that found in the literature.[52] The organic cation of $PW_{11}M$ started to decompose in the 150–200 °C range which was far above the temperature in the oxidation experiment.

Polyoxometalates are supposed to have remarkable hydrolytic stability and oxidative stability since they have good catalytic performances in oxidation of organic substrates with aqueous H_2O_2.[19–34] Although some researchers have demonstrated that the Keggin-type catalyst precursors, such as $[PW_{12}O_{40}]^{3-}$, $[PW_{11}O_{39}]^{7-}$ and $[PMo_{12}O_{40}]^{3-}$, are labile and can degrade to small active species in aqueous H_2O_2,[42–44] relevant research works paid little attention to the effect of H_2O_2 on the Keggin-type transition metal substituted polyoxometalates (TMSPs). In particular, catalyst stabilities were usually ignored in homogeneous catalysis for hydrocarbons oxidation.[23–25,29,33] Characterization techniques were restricted to IR, Raman and UV-Vis spectroscopy, and XRD patterns.[19,20,27,30–32] In addition, NMR spectra were seldom applied to characterize TMSPs due to the paramagnetic effect of transition metal.[34] The absence of chemical shift in ^{31}P NMR spectra (−247–147 ppm) of $PW_{11}M$ is attributed to the paramagnetic effect caused by the presence of transition metal ion (Co(II), Cu(II), Fe(III), Ni(II) and Mn(II)) (Figure S4a in the Supporting Information).

As was mentioned before, H_2O_2 to $PW_{11}M$ mole ratio has a significant influence on cyclohexene oxidation. To assess the effect of H_2O_2 on the catalyst stability, a series of characterization were carried out for $PW_{11}M$ and PW_{11} after treated with aqueous H_2O_2 in the absence of cyclohexene, including ^{31}P NMR, UV-Vis, FT-IR spectroscopy and elemental analysis (detailed in the Supporting Information). UV-Vis spectroscopic studies indicated a change in the oxidation state of manganese (from Mn(II) to Mn(III)) due to a new broad band at 488 nm (Figure S5 in the Supporting Information), which is attributed to a d-d electronic transition of Mn(III).[53]

The ^{31}P NMR spectra of $PW_{11}M$ and PW_{11} after treated with 250 equivalents of H_2O_2 are shown in Figure 2. Compared with the initial spectra (Figure S4a in the Supporting Information), two new chemical shifts were observed for $PW_{11}Co$, $PW_{11}Ni$, $PW_{11}Mn$ and PW_{11}, and only one chemical shift was found for $PW_{11}Cu$, while none for $PW_{11}Fe$. The chemical shift with satellites in the region of 2.7–3.0 ppm corresponds to PW_4 (Figure S1c in the Supporting Information), and another one around −15.3 ppm corresponds to PW_{12} (Figure S1a in the Supporting Information). Thus, we may conclude that $PW_{11}M$ (M = Co, Cu, Ni and Mn) could be decomposed into PW_4 (except for $PW_{11}Cu$) and PW_{12} in the presence of excess H_2O_2, at least, 250 equivalents of H_2O_2 (Scheme 1), and $PW_{11}Fe$ demonstrated excellent oxidative stability with H_2O_2. ICP measurements revealed that metal atoms released from the skeleton of $PW_{11}M$ (except for $PW_{11}Fe$) simultaneously during the decomposition. A similar detachment of substituting metals was observed in

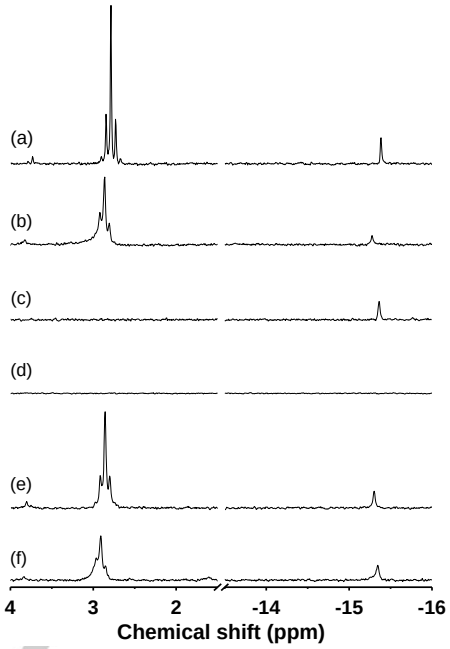

Figure 2. ^{31}P NMR spectra of (a) PW_{11}, (b) $PW_{11}Co$, (c) $PW_{11}Cu$, (d) $PW_{11}Fe$, (e) $PW_{11}Ni$ and (f) $PW_{11}Mn$ (10 mM) in CD_3CN/CH_2Cl_2 (50/50, vol%) after treated with 250 equivalents of H_2O_2.

vanadium-substituted phosphomolybdates catalyzed oxidation reactions with O_2 as oxidant.[54] The issue of metal leaching also existed in some complexes of transition metals for catalytic oxidation of cycloalkenes.[1,15] However, according to the ^{31}P NMR spectra measured after treated with 100 equivalents of H_2O_2 (Figure S4c in the Supporting Information), $PW_{11}M$ seemed to have good oxidative stability under low H_2O_2 to $PW_{11}M$ mole ratio since no additional chemical shift was detected.

FT-IR spectroscopic studies could further confirm the decomposition of PW_{11}. The FT-IR spectra obtained after treated with 250 equivalents of H_2O_2 in Figure S7a were consistent with the spectrum of PW_4 in Figure S6 in the Supporting Information, which indicates that most of PW_{11} were decomposed into PW_4 with H_2O_2. However, the FT-IR spectra of $PW_{11}M$ were nearly unchanged even after 24 hours in Figure S7b–f in the Supporting Information. It is reasonable to suppose that, unlike PW_{11}, only small amounts of $PW_{11}M$ were decomposed in the presence of H_2O_2 that could not be observed by UV-Vis and FT-IR spectroscopy but could be detected by ^{31}P NMR spectroscopy. Mono-substituted phosphotungstates showed better oxidative stability than the lacunary-type phosphotungstate (PW_{11}). Indeed, only PW_{11} was decomposed with 100 equivalents of H_2O_2 (Figure S4c in the Supporting Information).

Reaction pathways

Effect of radical scavenger. It is widely accepted that the allylic oxidation of cycloalkenes with O_2 proceeds through a radical

Accepted Manuscript

This article is protected by copyright. All rights reserved.

Table 2. The effect of radical scavenger on cyclohexene oxidation.[a]

Entry	Catalyst	Yield of products [%][b]		E_{H2O2} [%][c]
		1 + **2** + **3**	**4** + **5** + **6** + **7**	
1	–	0	0.3 (0.1)	90.8 (99.0)
2	$PW_{11}Co$	0	0.7 (2.6)	1.5 (70.1)
3	$PW_{11}Cu$	0	0.4 (0.7)	<1 (35.3)
4	$PW_{11}Fe$	0.1	18.5 (10.7)	61.3 (75.5)
5	$PW_{11}Ni$	0	32.2 (32.3)	84.1 (98.0)
6	$PW_{11}Mn$	0	4.6 (4.3)	9.4 (15.0)
7	PW_{11}	0	29.0 (27.7)	62.0 (80.1)
8	PW_4	0	41.5 (39.2)	94.2 (96.8)
9	PW_{12}	0	1.6 (2.0)	53.5 (98.4)

[a] Reaction conditions: catalyst (40 μmol), cyclohexene (20 mmol), H_2O_2 (10 mmol), BHT (2 mmol), CH_3CN (10 mL), 60 °C, 3 h. [b] Yield was determined by GC based on cyclohexene, 100 × (moles of **4**, **5**, **6** and **7**)/moles of initial cyclohexene; value in parentheses corresponds to the yield attaining without BHT. [c] Efficiency of H_2O_2 utilization; value in parentheses corresponds to the efficiency attaining without BHT.

mechanism in the liquid phase, and a hydroperoxide (ROOH) is produced as the primary product in free radical oxidation of cycloalkenes.[1,7,11,15,16] Simões and co-workers have demonstrated that the oxidation of cycloalkanes catalyzed by Keggin-type transition metal substituted polyoxotungstates with H_2O_2 involves a radical mechanism.[23–25] The allylic oxidation of cyclohexene also appeared to be a radical process in the presence of phosphotungstates and H_2O_2, as proved by the experiments carried out with 2,6-di-*tert*-butyl-4-methylphenol (BHT), a radical scavenger. As shown in Table 2 (yield details are listed in Table S1 in the Supporting Information), there was no allylic oxidation products (**1**, **2** and **3**) detected after addition of 2 mmol of BHT. While for $PW_{11}Fe$, a few yields of **1** and **2** were formed after addition of BHT. Non-radical processes may occur catalyzed by Fe-substituted polyoxometalates.[22]

On the contrary, the yields of **4**, **5**, **6** and **7** had little change or even increased after addition of BHT. As was discussed in the previous section, PW_4 will be formed with 250 equivalents of H_2O_2 for PW_{11} and $PW_{11}M$ (M =Co, Ni and Mn) which has high catalytic activity for epoxidation of alkenes,[44,50,51] as well as ketonization of alcohols and diols, oxidative cleavage of 1,2-diols and alkenes[51] based on tungsten-peroxo species through non-radical processes. Therefore, the epoxidation, ketonization and cleavage reactions could not be inhibited by the radical scavenger.

Kinetic study. To study a possible mechanism for the oxidation of cyclohexene catalyzed by $PW_{11}M$, experiments were carried out using different concentration of $PW_{11}Co$ with careful monitoring of the reaction products. The time-dependent conversion of cyclohexene and yields of products catalyzed by 1.6 mM $PW_{11}Co$ are plotted in Figure 3. The cyclohexene conversion increased slowly after 2 h due to the consumption of

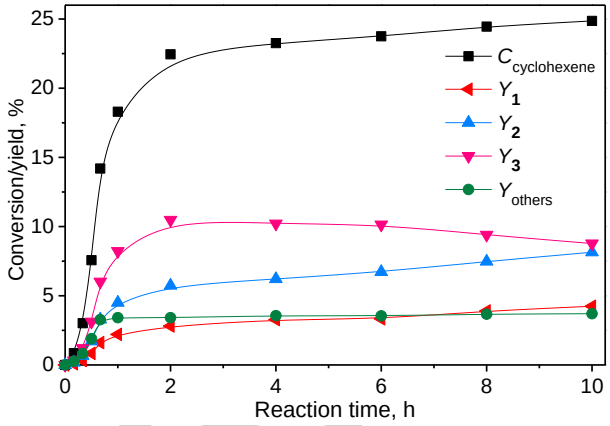

Figure 3. The time-dependent conversion of cyclohexene and yields of products catalyzed by 1.6 mM $PW_{11}Co$. Reaction conditions: $PW_{11}Co$ (20 μmol), cyclohexene (20 mmol), H_2O_2 (10 mmol), CH_3CN (10 mL), 60 °C.

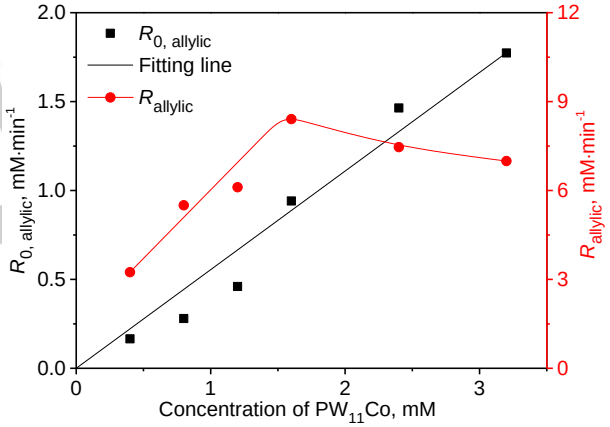

Figure 4. Dependence of reaction rates of allylic oxidation on concentration of $PW_{11}Co$. Reaction conditions: $PW_{11}Co$ (0.4–3.2 mM), cyclohexene (20 mmol), H_2O_2 (10 mmol), CH_3CN (10 mL), 60 °C. $R_{0,\ allylic}$ was the initial rate of allylic oxidation in induction period determined from the reaction profiles (Fig. S3); $R_{allylic}$ values were obtained by slope of the linear section after induction period

H_2O_2, and reached 24.9% after 10 h. The yield of **3** reached the highest at around 2 h and then decreased. The transformations of hydroperoxide resulted in the notable increase of yields of **1** and **2** after 2 h. Interestingly, the alcohol to ketone (**1**/**2**) molar ratio maintained at around 0.5 after 2 h. Besides, since the other products (**4**, **5**, **6** and **7**) derived from epoxidation were almost unchanged after 2 h, one can assume that the epoxidation primarily occurred at the initial stage of reaction. It is in good agreement with the observation that enough H_2O_2 to precursor molar ratio was essential to the formation of PW_4 and little epoxidation was observed until PW_4 was in appreciable concentration.[44]

The S-shaped time-dependent concentrations of allylic oxidation products catalyzed by $PW_{11}Co$ are shown in Figure S3 in the Supporting Information. About 10–50 min induction periods could be observed as concentration of $PW_{11}Co$ decreased from 3.2 mM to 0.4 mM. The initial rates of allylic

Accepted Manuscript

This article is protected by copyright. All rights reserved.

oxidation ($R_{0,\ allylic}$) in induction period were approximately first-order dependent on concentration of $PW_{11}Co$, as shown in Figure 4. The reaction rates of allylic oxidation ($R_{allylic}$) obtained by slope of the linear section after induction period increased with the increase in concentration of $PW_{11}Co$ and reached the maximum at around 1.6 mM, then decreased. Similar variation of oxidation rates with concentration of $PW_{11}Co$ was reported for the epoxidation of *trans*-stilbene with O_2/aldehyde involving radical species.[55] Vanadium-substituted phosphomolybdate ($H_5PV_2Mo_{10}O_{40}$) also showed similar behavior for the free radical oxidation of alkane with O_2 or O_2/aldehyde.[54,56] It is suggested that these polyoxometalates might behave as catalysts at their low concentrations and as inhibitors simultaneously at high concentrations.[54–56] The inhibiting effect of BHT, the predominant formation of cyclohexene hydroperoxide, the induction period and the bell-shaped dependence of the rate on the concentration of catalyst strongly conclude that the allylic oxidation of cyclohexene proceeds through a radical mechanism.

Detection of free radicals. In the transition metal-catalyzed oxidations of organic compounds with H_2O_2, represented by Fe complexes,[24,57] the hydroxyl radicals (HO•) and hydroperoxyl radicals (HOO•) initiated by transition metal is a predominant catalytic mechanism. The generated radicals were detected by EPR with 5,5-dimethyl-pyrroline-oxide (DMPO) as a spin trap to further confirm the radical mechanism of allylic oxidation of cyclohexene, as shown in Figure 5. Compared with the EPR spectrum using a Fenton reaction in acetonitrile solution (Figure 5f), the approximate 1:2:2:1 quartet was assigned to the DMPO/•OH adduct, suggesting the formation of HO• initiated by $PW_{11}M$. The three shoulder peaks were likely to be the signals of the DMPO/•OOH adduct.

Reaction pathways of cyclohexene oxidation. Based on the results observed in this work and other reports,[1,2,11,16,17,24] we can propose a mechanism for cyclohexene oxidation in the presence of $PW_{11}M$ and H_2O_2, as shown in Scheme 3. This tentative mechanism is composed of radical chain processes and non-radical processes. The EPR spectra (Figure 5) and the

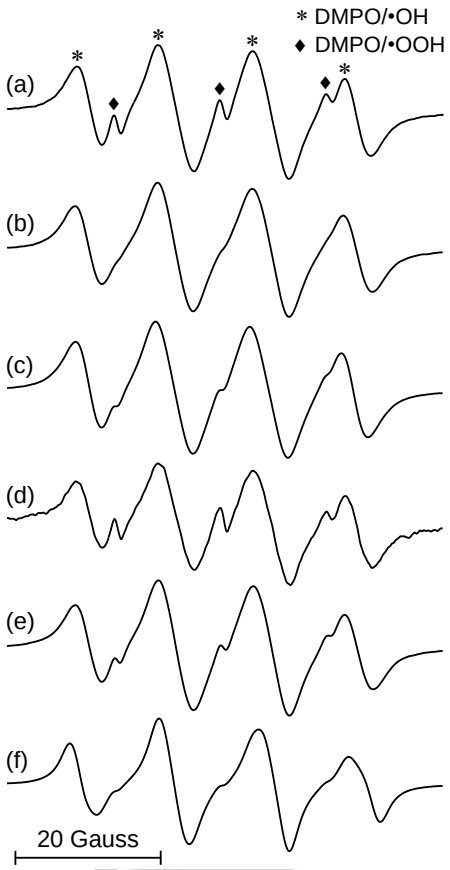

Figure 5. DMPO spin-trapping EPR spectra in acetonitrile solution in the presence of (a) $PW_{11}Co$, (b) $PW_{11}Cu$, (c) $PW_{11}Fe$, (d) $PW_{11}Ni$ and (e) $PW_{11}Mn$ (2 mM) and (f) ferric iron (1 mM) with H_2O_2 (100 mM) and DMPO (100 mM). Instrumental conditions: microwave power, 10 mW; modulation amplitude, 1.0 G; time constant, 0.082s; scan time, 5 min.

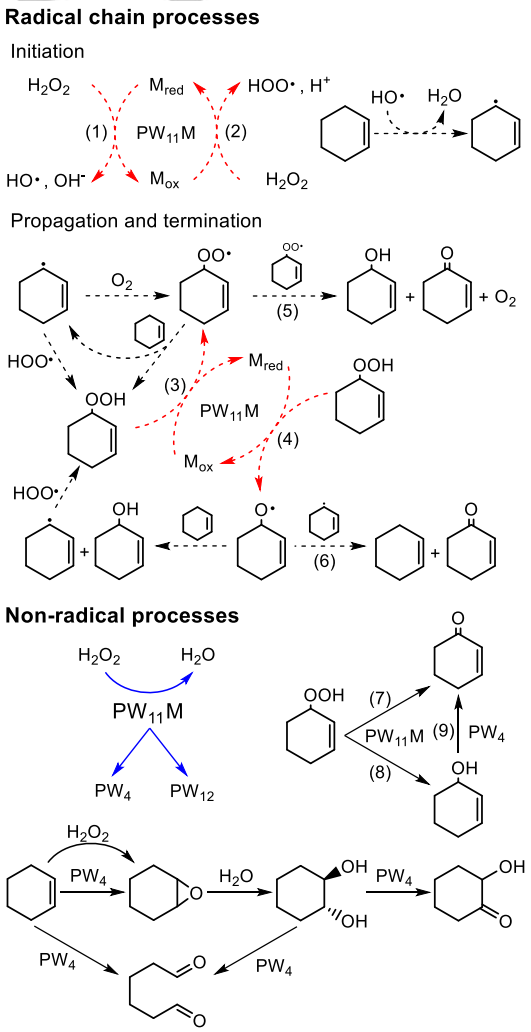

Scheme 3. Reaction pathways of cyclohexene oxidation in the presence of $PW_{11}M$ and H_2O_2: - - - radical chain pathway; - - - the well-known Haber-Weiss peroxide chain breakdown; M_{red}/M_{ox} = the reduced and oxidized forms of one-electron redox couple in $PW_{11}M$; —— non-radical pathway; —— the decomposition of $PW_{11}M$ with H_2O_2 (M = Co, Ni and Mn).

Accepted Manuscript

This article is protected by copyright. All rights reserved.

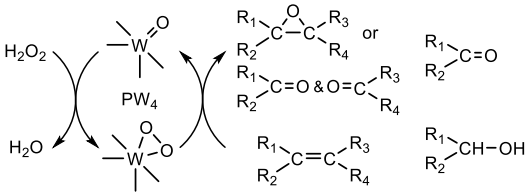

Scheme 4. Mechanism for epoxidation, ketonization and cleavage reactions catalyzed by PW_4. Adapted from ref. 42, 44, 50 and 51.

different catalytic performances observed from analogous structural $PW_{11}M$, PW_{11} and PW_{12} suggests that transition metal centers are the catalytic active sites for the radical chain reactions, and it is tungsten-peroxo species in PW_4 that are responsible for the epoxidation, ketonization and cleavage reactions (Scheme 4). NMR spectroscopic studies revealed the important role of PW_4 in cyclohexene oxidation which has been well discussed by Duncan et al.[44] The chemical shift of PW_4 in ^{31}P NMR spectrum was disappeared after the addition of cyclohexene (Figure S8 in the Supporting Information).

A decrease in induction period with the increase in concentration of $PW_{11}Co$ (Figure S3 in the Supporting Information), and the first-order dependence of the initial rate on concentration of $PW_{11}Co$ (Figure 4) indicate that $PW_{11}Co$ plays a critical role in the initiation of the radical chain processes. The induction period is required to build up sufficient chain carriers such as cyclohexenyl and cyclohexenyl peroxy radicals by the reaction among $PW_{11}M$, H_2O_2 and cyclohexene. The initial step in this radical chain processes involves the well-known Haber-Weiss peroxide chain breakdown[17] for the transformation of H_2O_2 to give HO• and HOO• based on the M_{red}/M_{ox} redox steps (1) and (2), as proved by Figure 5. The homolytic decomposition of hydroperoxide also depends on the M_{red}/M_{ox} redox cycling via steps (3) and (4). The rates of these four steps roughly correlate with the redox potential of M_{red}/M_{ox} couple which can be influenced by solvent and coordination environment,[11,17] and result in the different catalytic performances of $PW_{11}M$ for allylic oxidation. The radical processes which occurred during the PW_{11}, PW_4 and PW_{12} catalyzed oxidation reactions (Table 1, entries 7, 8 and 9) are likely attributed to the W(VI)/W(V) redox reactions.[58]

The initial generation of cyclohexenyl radicals is a key step in the allylic oxidation of cyclohexene. The HO• generated via step (1) then carries out hydrogen abstraction on the allylic C–H bond of cyclohexene to produce the active cyclohexenyl radical. The cyclohexenyl radicals could be converted to cyclohexene hydroperoxide with HOO• and cyclohexenyl peroxy radical with O_2 derived from the dismutation of H_2O_2. We observed a sharp decrease in efficiency of H_2O_2 utilization in the presence of BHT (Table 2), which indicates that the allylic oxidation was inhibited by BHT, most likely, because of the interaction of the radical scavenger with HO• and HOO•. Main chain termination steps (5) and (6) are shown in Scheme 3 according to the Haber-Weiss process.[7,11,17]

In general, the alcohol to ketone (A/K) molar ratio and selectivity to hydroperoxide should be an important consideration for the radical-driven oxidation of cyclohexene,[1,9,16] which can reflect different oxidation pathways. In non-radical processes, the heterolytic decomposition of cyclohexene hydroperoxide leading to produce 2-cyclohexen-1-ol (**1**) and 2-cyclohexen-1-one (**2**) occurs catalyzed by $PW_{11}M$ through non-radical processes. The heterolytic decomposition may involve dehydration and/or disproportionation reactions via step (7) and step (8), respectively, which is considered to happen in the presence of some complexes of transition metals, like Cu, Cr and Fe catalysts.[1,15] Co^{2+} active sites are also proved to be required to achieve the efficient decomposition of tetralinhydroperoxide.[59] The observed difference in the alcohol to ketone (**1**/**2**) molar ratio and selectivity to hydroperoxide (**3**) (Table S1 in the Supporting Information) can be associated with the catalytic selectivity and activity of $PW_{11}M$ for the decomposition of hydroperoxide. In addition to $PW_{11}Cu$, $PW_{11}M$ (M = Co, Fe, Ni and Mn) showed activity to favor the dehydration of hydroperoxide. The unusual low **1**/**2** molar ratio attained by PW_{11} and PW_4 is attributed to the ketonization catalyzed by tungsten-peroxo species.[42,51] Particularly, the oxidation of **1** via step (9) would occur under high H_2O_2 to $PW_{11}M$ mole ratio conditions for $PW_{11}Co$, $PW_{11}Ni$ and $PW_{11}Mn$.

In summary, allylic oxidation and epoxidation proceed through different reaction pathways based on transition metals and tungsten-peroxo species, respectively. Allylic oxidation predominately occurs under low H_2O_2 to $PW_{11}M$ mole ratio conditions when the Keggin-type primary structure is stable with H_2O_2. However, high H_2O_2 to $PW_{11}M$ mole ratio conditions will lead to the decomposition of $PW_{11}M$ and accelerate the undesirable decomposition of H_2O_2. Epoxidation is promoted by catalyst precursors of $PW_{11}M$ (M=Co, Ni, Mn). Allylic oxidation and epoxidation occur simultaneously due to the formation of PW_4. Thus, low H_2O_2 to $PW_{11}M$ mole ratio conditions (e.g. H_2O_2:$PW_{11}M$ = 100:1) are suggested to improve catalyst stability

Table 3. Catalytic performances of $PW_{11}Co$ in cyclohexene oxidation with H_2O_2[a] in comparison with other catalysts using acetonitrile as solvent.

Catalysts	Oxidant	T [°C]	t [h]	$C_{cyclohexene}$ [%]	$S_{allylic}$ [%]	TOF [h^{-1}][b]	Ref.
$PW_{11}Co$	H_2O_2	60	10	27.9	90.4	27.90	This work
Cu-amp-AMPS[c]	H_2O_2[d]	50	10	48	100	11.46	[60]
	TBHP	50	10	79	96	18.20	[60]
Cu-cationic salphend[e]	O_2	78	16	100	88.3	6.25	[10]
Fe(III)/SiO_2	O_2	58	10	33.7	95.3	6.70	[61]
	O_2	78	10	98.1	95	19.60	[61]
Co-MOF[f]	O_2	35	24	35	94.3	1.15	[62]

[a] Reaction conditions: $PW_{11}Co$ (40 μmol), cyclohexene (40 mmol), CH_3CN (20 mL); 4 mmol H_2O_2 were added initially, and then H_2O_2 were fed with a rate of 2.4 mmol·h^{-1}. [b] Turnover frequency (TOF) = moles of substrate converted per mole of catalyst per hour; moles of catalyst were based on transition metal. [c] Immobilized Schiff base copper complex, H_2-amp = N-(hydroxyphenyl)salicyldimine; AMPS = aminopropyl silica. [d] 40% acetic acid in acetonitrile was used as solvent. [e] Cu-[cationic salphen][PF_6^-]$_2$. [f] [Co_4O(bdpb)$_3$], H_2-bdpb = 1,4-bis[(3,5-dimethyl)-pyrazol-4-yl]benzene.

Accepted Manuscript

This article is protected by copyright. All rights reserved.

H_2O_2 utilization efficiency and allylic oxidation selectivity for cyclohexene oxidation catalyzed by $PW_{11}M$. As shown in Table 3, $PW_{11}Co$ showed outstanding catalytic performances in allylic oxidation of cyclohexene in comparison with other catalysts using acetonitrile as solvent.

Conclusions

The Keggin-type transition metal substituted phosphotungstates ($PW_{11}M$, M = Co, Cu, Fe, Ni and Mn) studied in this work are proved to be active catalysts for the oxidation of cyclohexene with H_2O_2 in homogeneous phase, and afford abundant oxidation products. $PW_{11}Co$ shows the highest catalytic activity for allylic oxidation among the $PW_{11}M$. The H_2O_2 to $PW_{11}M$ mole ratio has a significant effect on the oxidative stability of $PW_{11}M$ and the reaction selectivity. Different decomposition behaviors of $PW_{11}M$ were observed in the presence of excess H_2O_2. The ^{31}P NMR spectra clearly showed the decomposition of $PW_{11}M$ (M = Co, Cu, Ni and Mn) with 250 equivalents of H_2O_2. The formation of PW_4 is responsible for the dramatic decrease of selectivity to allylic oxidation products under high H_2O_2 to $PW_{11}M$ mole ratio conditions, and leads to the occurrence of epoxidation, ketonization and cleavage reactions.

The selective inhibiting effect of a radical scavenger (BHT) on allylic oxidation, EPR spectra and kinetic data indicate the radical mechanism of allylic oxidation of cyclohexene, while the oxidation of C=C double bond proceeds through non-radical pathways. Transition metals and tungsten-peroxo species are two kinds of active sites for generating free radicals and activating C=C double bond, respectively.

Experimental Section

Materials

$Na_2WO_4 \cdot 2H_2O$, $Na_2HPO_4 \cdot 12H_2O$, $H_3PW_{12}O_{40} \cdot xH_2O$, nitrate salts of Co(II), Cu(II), Fe(III), Ni(II), Mn(II), tetrabutylammonium bromide and tetrabutylammonium chloride used in synthesis of phosphotungstates were purchased from Tianjin Guangfu Fine Chemical Research Institute. CD_3CN (99.8% D) was purchased from Sigma-Aldrich. Cyclohexene was of highest purity from Shanghai Aladdin Bio-Chem Technology Co., Ltd. and used without further purification. Hydrogen peroxide was used as 40–50 wt% solution in water and its exact strength at the time of usage was determined by the ceric sulphate method[63]. Other reagents used were analytical grade available from commercial sources.

Characterization techniques

Elemental analysis for phosphorus, tungsten and transition metal was performed by the inductively coupled plasma optical emission spectroscopy (ICP-OES) on a Varian Vista-MPX ICP instrument. Thermogravimetric analysis (TGA) was carried out on a Mettler Toledo TGA/DSC 1 STAR^e System up to 700 °C in air at a heating rate of 10 °C/min. Infrared spectra were measured on a Nicolet Nexus FT-IR spectrometer with KBr pellets in the range of 400–4000 cm^{-1}, as well as a ReactIR 15 instrument from Mettler Toledo AutoChem fitted with an AgX optic fiber and Dicomp (Diamond Composite) insertion probe in the range of 650–3000 cm^{-1}. Ultraviolet visible (UV-Vis) absorption spectra were measured at ambient temperature on a Shimadzu UV-2550 spectrometer using the 1 cm quartz cell. ^{31}P nuclear magnetic resonance (NMR) spectra were recorded on a Bruker AVANCE III instrument in CD_3CN/CH_2Cl_2 (50/50, vol%) at 162 MHz in the range of −247–147 ppm, with 85% H_3PO_4 as an external standard. Electron paramagnetic resonance (EPR) signals of radicals trapped by 5,5-dimethyl-pyrroline-oxide (DMPO) were recorded at ambient temperature on a Bruker EMXplus-6/1 spectrometer. Gas chromatography (GC) analyses were carried out on an Agilent 7890A GC equipped with a flame ionization detector and a HP-Wax capillary column (internal diameter 0.25 mm, length 60 m). Mass spectra were recorded on an Agilent 6890N-5975 inert GC-MS equipped with a HP-5MS capillary column (internal diameter 0.25 mm, length 30 m).

Preparation of phosphotungstates

The tetrabutylammonium salts, $(TBA)_4H_x[PW_{11}M(L)O_{39}] \cdot nH_2O$, M = Co(II) Cu(II), Fe(III), Ni(II), Mn(II), L = H_2O or absence,[23] $(TBA)_3[PW_{12}O_{40}]$,[64] $(TBA)_4H_3[PW_{11}O_{39}]$,[65] and $(TBA)_3[PW_4O_{24}]$,[43] were synthesized with procedures described in the literature, and characterized by elemental and thermal analysis, FT-IR, UV-Vis and ^{31}P NMR spectroscopy, confirming the synthesis of the desired compound. The results of characterization are detailed in the Supporting Information.

Cyclohexene oxidation

Oxidation of cyclohexene was carried out in a 25 mL two-necked round bottom flask equipped with a water condenser and a magnetic stir bar. Typically, 20 mmol cyclohexene, 4–20 mmol H_2O_2 in aqueous solution, 3–60 μmol phosphotungstate, and 10 mL acetonitrile were fed into the reactor and then immersed in a previously heated water bath at desired temperature under vigorous stirring. After reaction, the reactor was cooled to room temperature immediately. The liquid product was extracted with dichloromethane, dried with magnesium sulfate and quantified by GC techniques with toluene as an internal standard. Cyclohexene hydroperoxide was treated with triphenylphosphine (PPh_3) prior to the GC analyses, and it was determined according to method described in the literature.[47] Other products were known compounds and identified by comparison of their retention times and mass spectra with those of authentic samples.

For determination of unused H_2O_2 and hydroperoxide produced after oxidation experiment, the titration of peroxides was carried out using the ceric sulphate method[63]. The sample was accurately weighed and quickly dissolved in dilute sulphuric acid. The solution was titrated against 100 mM ceric sulphate solution, using ferroin as indicator.

Acknowledgements

This work was supported by the National Natural Science Foundation of China (NSFC 21276180).

Keywords: transition metal • phosphotungstates • allylic oxidation • reaction pathways • radical mechanism

[1] I. Y. Skobelev, A. B. Sorokin, K. A. Kovalenko, V. P. Fedin, O. A. Kholdeeva, *J. Catal.* **2013**, *298*, 61–69.
[2] P. Bujak, P. Bartczak, J. Polanski, *J. Catal.* **2012**, 295, 15–21.

Accepted Manuscript

This article is protected by copyright. All rights reserved.

[3] F. P. da Silva, R. V. Goncalves, L. M. Rossi, *J. Mol. Catal. A: Chem.* **2017**, *426*, 534–541.
[4] A. Dhakshinamoorthy, M. Alvaro, H. Garcia, *J. Catal.* **2012**, *289*, 259–265.
[5] D. Yang, T. Jiang, T. Wu, P. Zhang, H. Han, B. Han, *Catal. Sci. Technol.* **2016**, *6*, 193–200.
[6] M. Boualleg, K. Guillois, B. Istria, L. Burel, L. Veyre, J. Basset, C. Thieuleux, V. Caps, *Chem. Commun.* **2010**, *46*, 5361–5363.
[7] Z. Cai, M. Zhu, J. Chen, Y. Shen, J. Zhao, Y. Tang, X. Chen, *Catal. Commun.* **2010**, *12*, 197–201.
[8] F. P. Silva, M. J. Jacinto, R. Landers, L. M. Rossi, *Catal. Lett.* **2011**, *141*, 432–437.
[9] S. E. Dapurkar, H. Kawanami, K. Komura, T. Yokoyama, Y. Ikushima, *Appl. Catal. A: Gen.* **2008**, *346*, 112–116.
[10] A. Abdolmaleki, S. R. Adariani, *Catal. Commun.* **2015**, *59*, 97–100.
[11] Y. Fu, D. Sun, M. Qin, R. Huang, Z. Li, *RSC Adv.* **2012**, *2*, 3309–3314.
[12] D. Jiang, T. Mallat, D. M. Meier, A. Urakawa, A. Baiker, *J. Catal.* **2010**, *270*, 26–33.
[13] D. Rutkowska-Zbik, M. Witko, E. M. Serwicka, *Catal. Today* **2011**, *169*, 10–15.
[14] E. F. Murphy, T. Mallat, A. Baiker, *Catal. Today* **2000**, *57*, 115–126.
[15] Y. Chang, Y. Lv, F. Lu, F. Zha, Z. Lei, *J. Mol. Catal. A: Chem.* **2010**, *320*, 56–61.
[16] Y. Cao, H. Yu, F. Peng, H. Wang, *ACS Catal.* **2014**, *4*, 1617–1625.
[17] R. A. Sheldon, J. K. Kochi, *Metal-Catalyzed Oxidations of Organic Compounds*, Academic Press, New York, **1981**, pp. 33–70.
[18] N. Mizuno, K. Yamaguchi, K. Kamata, *Coordin. Chem. Rev.* **2005**, *249*, 1944–1956.
[19] S. S. Balula, L. Cunha-Silva, I. C. M. S. Santos, A. C. Estrada, A. C. Fernandes, J. A. S. Cavaleiro, J. Pires, C. Freire, A. M. V. Cavaleiro, *New J. Chem.* **2013**, *37*, 2341–2350.
[20] S. S. Balula, I. C. M. S. Santos, L. Cunha-Silva, A. P. Carvalho, J. Pires, C. Freire, J. A. S. Cavaleiro, B. de Castro, A. M. V. Cavaleiro, *Catal. Today* **2013**, *203*, 95–102.
[21] S. Wang, G. Yang, *Chem. Rev.* **2015**, *115*, 4893–4962.
[22] N. Mizuno, C. Nozaki, I. Kiyoto, M. Misono, *J. Am. Chem. Soc.* **1998**, *120*, 9267–9272.
[23] M. M. Q. Simões, C. M. M. Conceição, J. A. F. Gamelas, P. M. D. N. Domingues, A. M. V. Cavaleiro, J. A. S. Cavaleiro, A. J. V. Ferrer-Correia, R. A. W. Johnstone, *J. Mol. Catal. A: Chem.* **1999**, *144*, 461–468.
[24] M. S. S. Balula, I. C. M. S. Santos, M. M. Q. Simões, M. G. P. M. S. Neves, J. A. S. Cavaleiro, A. M. V. Cavaleiro, *J. Mol. Catal. A: Chem.* **2004**, *222*, 159–165.
[25] M. M. Q. Simões, I. C. M. S. Santos, M. S. S. Balula, J. A. F. Gamelas, A. M. V. Cavaleiro, M. G. P. M. S. Neves, J. A. S. Cavaleiro, *Catal. Today* **2004**, *91–92*, 211–214.
[26] K. Kamata, K. Yonehara, Y. Nakagawa, K. Uehara, N. Mizuno, *Nat. Chem.* **2010**, *2*, 478–483.
[27] A. C. Estrada, I. C. M. S. Santos, M. M. Q. Simões, M. G. P. M. S. Neves, J. A. S. Cavaleiro, A. M. V. Cavaleiro, *Appl. Catal. A: Gen.* **2011**, *392*, 28–35.
[28] Y. Wang, K. Kamata, R. Ishimoto, Y. Ogasawara, K. Suzuki, K. Yamaguchi, N. Mizuno, *Catal. Sci. Technol.* **2015**, *5*, 2602–2611.
[29] P. A. Shringarpure, A. Patel, *Synth. React. Inorg. M.* **2015**, *45*, 397–406.
[30] J. Hu, K. Li, W. Li, F. Ma, Y. Guo, *Appl. Catal. A: Gen.* **2009**, *364*, 211–220.
[31] S. Rana, S. Mallick, L. Mohapatra, G. B. B. Varadwaj, K. M. Parida, *Catal. Today* **2012**, *198*, 52–58.
[32] S. Pathan, A. Patel, *Ind. Eng. Chem. Res.* **2013**, *52*, 11913–11919.
[33] T. A. G. Duarte, A. C. Estrada, M. M. Q. Simões, I. C. M. S. Santos, A. M. V. Cavaleiro, M. G. P. M. S. Neves, J. A. S. Cavaleiro, *Catal. Sci. Technol.* **2015**, 5, 351–363.
[34] S. Pathan, A. Patel, *Appl. Catal. A: Gen.* **2013**, *459*, 59–64.
[35] N. Mizuno, C. Nozaki, I. Kiyoto, M. Misono, *J. Catal.* **1999**, *182*, 285–288.
[36] O. A. Kholdeeva, T. A. Trubitsina, M. N. Timofeeva, G. A. Maksimov, R. I. Maksimovskaya, V. A. Rogov, *J. Mol. Catal. A: Chem.* **2005**, *232*, 173–178.
[37] O. A. Kholdeeva, R. I. Maksimovskaya, *J. Mol. Catal. A: Chem.* **2007**, *262*, 7–24.
[38] N. V. Maksimchuk, M. N. Timofeeva, M. S. Melgunov, A. N. Shmakov, Y. A. Chesalov, D. N. Dybtsev, V. P. Fedin, O. A. Kholdeeva, *J. Catal.* **2008**, *257*, 315–323.
[39] N. V. Maksimchuk, M. S. Meigunov, Y. A. Chesalov, J. Mrowiec-Białoń, A. B. Jarzębski, O. A. Kholdeeva, *J. Catal.* **2007**, *246*, 241–248.
[40] J. Tong, W. Wang, L. Su, Q. Li, F. Liu, W. Ma, Z. Lei, L. Bo, *Catal. Sci. Technol.* **2017**, *7*, 222–230.
[41] N. M. Gresley, W. P. Griffith, A. C. Laemmel, H. I. S. Nogueira, B. C. Parkin, *J. Mol. Catal. A: Chem.* **1997**, *117*, 185–198.
[42] Z. Weng, J. Wang, X. Jian, *Catal. Commun.* **2008**, *9*, 1688–1691.
[43] C. Aubry, G. Chottard, N. Platzer, J. M. Brégeault, R. Thouvenot, F. Chauveau, C. Huet, H. Ledon, *Inorg. Chem.* **1991**, *30*, 4409–4415.
[44] D. C. Duncan, R. C. Chambers, E. Hecht, C. L. Hill, *J. Am. Chem. Soc.* **1995**, *117*, 681–691.
[45] W. Zhao, Y. Ding, *React. Kinet. Mech. Cat.* **2013**, *109*, 509–524.
[46] G. B. Shulpin, G. V. Nizova, *React. Kinet. Catal. Lett.* **1992**, *48*, 333–338.
[47] G. B. Shul'pin, *J. Mol. Catal. A: Chem.* **2002**, *189*, 39–66.
[48] J. Gao, Y. Chen, B. Han, Z. Feng, C. Li, N. Zhou, S. Gao, Z. Xi, *J. Mol. Catal. A: Chem.* **2004**, 210, 197–204.
[49] C. Venturello, R. D'Aloisio, J. C. J. Bart, M. Ricci, *J. Mol. Catal.* **1985**, *32*, 107–110.
[50] C. Venturello, R. D'Aloisio, *J. Org. Chem.* **1988**, *53*, 1553–1557.
[51] Y. Ishii, K. Yamawaki, T. Ura, H. Yamada, T. Yoshida, M. Ogawa, *J. Org. Chem.* **1988**, *53*, 3587–3593.
[52] J. A. Gamelas, F. A. S. Couto, M. C. N. Trovão, A. M. V. Cavaleiro, J. A S. Cavaleiro, J. D. P. de Jesus, *Thermochim. Acta* **1999**, *326*, 165–173.
[53] C. M. Tourné, G. F. Tourné, S. A. Malik, T. J. R. Weakley, *J. Inorg. Nucl Chem.* **1970**, *32*, 3875–3890.
[54] S. Shinachi, M. Matsushita, K. Yamaguchi, N. Mizuno, *J. Catal.* **2005**, *233*, 81–89.
[55] O. A. Kholdeeva, V. A. Grigoriev, G. M. Maksimov, M. A. Fedotov, A. V. Golovin, K. I. Zamaraev, *J. Mol. Catal. A: Chem.* **1996**, *114*, 123–130.
[56] A. M. Khenkin, A. Rosenberger, R. Neumann, *J. Catal.* **1999**, *182*, 82–91.
[57] G. B. Shul'pin, G. V. Nizova, Y. N. Kozlov, L. G. Cuervo, G. Süss-Fink, *Adv. Synth. Catal.* **2004**, *346*, 317–332.
[58] I. C. M. S. Santos, F. A. A. Paz, M. M. Q. Simões, M. G. P. M. S. Neves J. A. S. Cavaleiro, J. Klinowski, A. M. V. Cavaleiro, *Appl. Catal. A: Gen.* **2008**, *351*, 166–173.
[59] F. X. L. i Xamena, O. Casanova, R. G. Tailleur, H. Garcia, A. Corma, *J. Catal.* **2008**, *255*, 220–227.
[60] S. Mukherjee, S. Samanta, B. C. Roy, A. Bhaumik, *Appl. Catal. A: Gen.* **2006**, *301*, 79–88.
[61] J. Mao, X. Hu, H. Li, Y. Sun, C. Wang, Z. Chen, *Green Chem.* **2008**, *10* 827–831.
[62] M. Tonigold, Y. Lu, A. Mavrandonakis, A. Puls, R. Staudt, J. Möllmer, J. Sauer, D. Volkmer, *Chem. Eur. J.* **2011**, *17*, 8671–8695.
[63] A. I. Vogel, *A Text-Book of Quantitative Inorganic Analysis Including Elementary Instrumental Analysis*, Longmans, London, **1961**, pp. 325–326.
[64] C. Rocchiccioli-Deltcheff, M. Fournier, R. Franck, R. Thouvenot, *Inorg. Chem.* **1983**, *22*, 207–216.
[65] E. Radkov, R. H. Beer, *Polyhedron* **1995**, *14*, 2139–2143.

Accepted Manuscript

This article is protected by copyright. All rights reserved.

10.1002/cctc.201700856

Table of Contents

FULL PAPER

Reaction pathways of cyclohexene oxidation: Homogeneous catalytic oxidations of cyclohexene by transition metal substituted phosphotungstates with hydrogen peroxide were explored. Allylic oxidation and epoxidation proceed via radical pathways based on transition metals and via non-radical pathways based on PW_4, respectively.

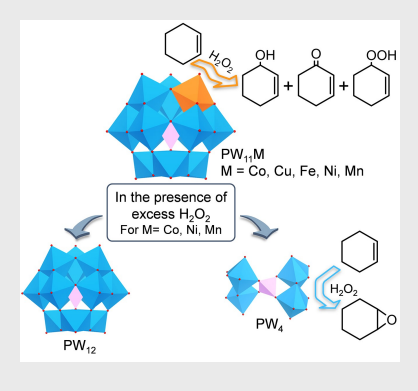

Yuexiao Song, Feng Xin, Lexiang Zhang, Yong Wang*

Page No. – Page No.

Oxidation of cyclohexene in the presence of transition metal substituted phosphotungstates and hydrogen peroxide: catalysis and reaction pathways

WILEY-VCH
Accepted Manuscript

This article is protected by copyright. All rights reserved.